

**EFFECTS OF SPACE WEATHERING ON REFLECTANCE SPECTRA OF UREILITES: FIRST STUDIES.** C. A. Goodrich<sup>1</sup>, J. Gillis-Davis<sup>2</sup>, E. Cloutis<sup>3</sup>, D. Applin<sup>3</sup>, D. Takir<sup>4</sup>, C. Hibbitts<sup>5</sup>, R. Christoffersen<sup>6</sup>, M. Fries<sup>7</sup>, R. Klima<sup>5</sup> and S. Decker<sup>8</sup>. <sup>1</sup>Lunar and Planetary Institute, USRA, Houston, TX 77058 USA ([goodrich@lpi.usra.edu](mailto:goodrich@lpi.usra.edu)); <sup>2</sup>HIGP, Univ. HI Manoa, Honolulu HI USA ([gillis@higp.hawaii.edu](mailto:gillis@higp.hawaii.edu)); <sup>3</sup>Dept. Geogr., Univ. Winnipeg, Winnipeg, MB Canada; <sup>4</sup>SETI Institute, Mountain View CA USA. <sup>5</sup>Johns Hopkins Univ./APL, Laurel, MD USA; <sup>6</sup>Jacobs, NASA JSC, Houston TX USA; <sup>7</sup>ARES, NASA JSC, Houston TX USA; <sup>8</sup>Oberwesel Germany.

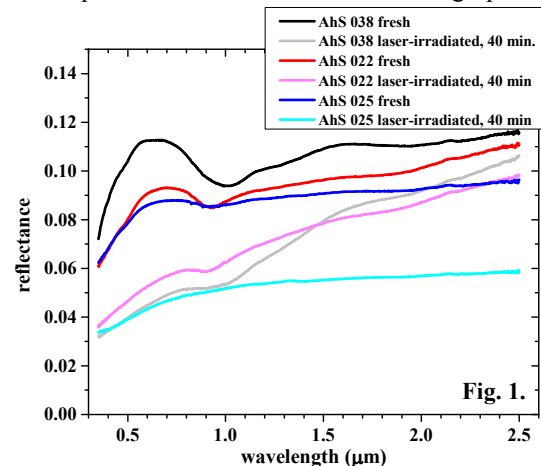
**Introduction:** Ureilites are differentiated meteorites (ultramafic rocks interpreted to be mantle residues) that contain as much carbon as the most carbon-rich carbonaceous chondrites (CCs) [1,2]. Reflectance spectra of ureilites are similar to those of some CCs [3]. Hence, ureilitic asteroids may accidentally be categorized as primitive because their spectra could resemble those of C-complex asteroids, which are thought to be CC-like. We began spectral studies of progressively laser-weathered ureilites with the goals of predicting UV-VIS-IR spectra of ureilitic asteroids, and identifying features that could distinguish differentiated from primitive dark asteroids. Space weathering has not previously been studied for ureilites, and, based on space weathering studies of CCs and other C-rich materials [4-8], it could significantly alter their reflectance spectra.

**Samples and Methods:** We are using ureilitic samples from the 2008 fall Almahata Sitta [2,9,10], because they have the lowest degree of weathering of any ureilites available and represent a range of ureilite types. The three samples available for initial studies were: MS-MU-038, -022 and -025. A chip from each sample was used for a thin section. The remainder of each sample was ground and dry-sieved to <75  $\mu\text{m}$  grain size to simulate regolith [6,11]. Thin sections were studied by FE-SEM and EMPA. Quarter-gram aliquots of the original powders were studied by UV-IR and Raman spectroscopy, XRD and FE-SEM. Space weathering of powders was simulated by pulsed laser irradiation [5,12]. Spectra were measured after 6000, 12000, 24000, 36000, and 48000 accumulated laser shots – an estimated exposure age of 800,000 years. The irradiated powders were studied with the same techniques as the non-irradiated powders.

**Results:** The three samples show a range of ureilite primary features and shock levels. MS-MU-038 is a coarse-grained (~1-2 mm), olivine-rich (Fo ~76) ureilite of low shock level with euhedral graphite. MS-MU-022 is a medium-grained (~0.1-0.3 mm), olivine (Fo ~89) + orthopyroxene (mg# ~90, Wo 4.8) ureilite of medium shock level. Pyroxenes show shock lamellae and shock-smelting. Both -038 and -025 contain graphite, metal and sulfide in lower abundance than many ureilites. MS-MU-025 is a fine-grained ( $\leq 20 \mu\text{m}$ ), ureilite. It consists of olivine-rich and

pyroxene-rich domains that represent originally large crystals. Both phases have been extensively shock-smelted [13] and recrystallized and contain finely-dispersed metal and sulfide. Cores of olivine-rich domains are Fo 79 but recrystallized olivine has Fo as high as 99. Metal and sulfide also occur as large veins.

Pre-irradiation reflectance spectra of all samples show low albedo (0.08-0.11 % at 0.7  $\mu\text{m}$ ) and a steep UVVIS (~0.3-0.6  $\mu\text{m}$ ) continuum (Fig. 1). The absence of terrestrial iron (hydr)oxides is shown by the absence of bands near 0.22, 0.5 and 0.9  $\mu\text{m}$ . MS-MU-038 exhibits olivine absorption between 1.05 and 1.10  $\mu\text{m}$ . MS-MU-022 exhibits the characteristic two absorption bands of pyroxene, near 1  $\mu\text{m}$  and 2  $\mu\text{m}$ . Its overall lower reflectance relative to -038 could be due to higher shock level. Both -038 and -022 are darker and redder than pure olivine and/or pyroxene, possibly due to the presence of fine-grained metal/sulfide. MS-MU-025 shows the lowest overall reflectance and shallowest absorptions, probably due to high shock level and high metal/sulfide abundance. In the UV, all samples show a 0.23  $\mu\text{m}$  peak attributable to graphite. Raman spectra show the D and G bands of graphite.



In response to laser irradiation, VNIR spectra of samples -038 and -022 became increasingly redder and darker, and lost spectral contrast (Fig. 1). The change in absolute reflectance at 740 nm, and the overall reddening, was greater for -038. The spectrum of -025 became darker and lost what little spectral contrast it had (Fig. 1). In -038, the Raman graphite peaks broadened and the D band became as intense as the G

band, indicating disordering. FE-SEM of the irradiated powders of all 3 samples (Fig. 2) shows significant melting of grain surfaces, with production of micro- and nano-phase Fe metal and sulfide spherules.

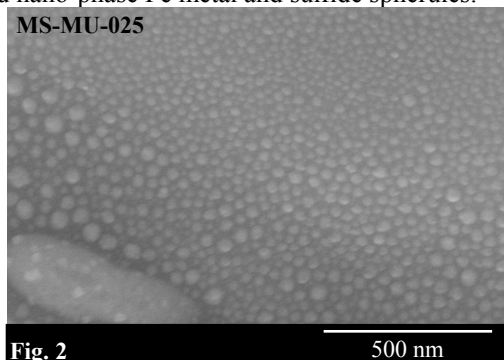


Fig. 2

**Discussion:** Although ureilites have a simple mineralogy [2,16], their reflectance spectra are diverse [3] due to variations in olivine/pyroxene ratio, silicate compositions, abundances of graphite, metal and sulfide, and shock level (with associated properties grain size, texture, and composition). The effects of each of these variables on reflectance spectra must be understood as a baseline for studying space weathering of ureilites. AhS has a large proportion of highly shocked, fine-grained porous ureilites [9,15], supporting the interpretation that asteroid 2008 TC<sub>3</sub> (which spawned AhS) represents ureilitic regolith [2,15]. Some of those samples have very flat dark spectra similar to C and B asteroids [14] but lacking a 2.7  $\mu\text{m}$  band of hydrated phases. However, one AhS sample is a breccia of C1, ureilitic, and OC materials, and shows a flat, dark spectrum with a strong 2.7 band [15,22]. None of the samples we studied here are of these types, though -025 is the closest (most shocked). Sample -038 is probably an interior mantle sample.

Our results show that space weathering causes significant changes in UV-IR spectra of ureilites. Comparing VNIR spectra of the irradiated samples with spectral parameters for SMASS asteroid classes (Fig. 3) shows that with increased laser weathering all 3 samples move away from C- and B- class asteroids and toward X, T and D asteroids. These results suggest that asteroid 2008 TC<sub>3</sub>, which had a spectrum resembling C-complex asteroids (Fig. 3b), was not significantly space-weathered, as discussed by [14] and consistent with an absence of solar gases [19,20].

Based on this preliminary work and other spectral studies of AhS [14,15,22], we infer that non-space weathered ureilitic regolith (represented by AhS fine-grained and breccia samples) may resemble C-complex asteroids in reflectance spectra. However, space weathered ureilitic material is more likely to resemble D, T or some X class asteroids. Systematic study of the effects of space weathering on the full range of ureilite

types is needed to derive criteria for distinguishing differentiated from primitive dark asteroids.

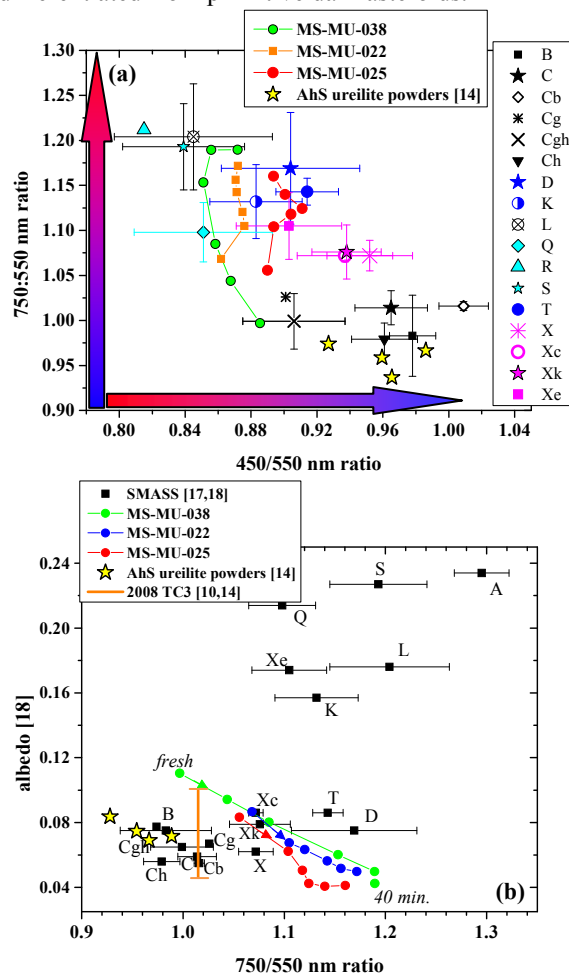


**Fig. 3.** Spectral parameters for mean SMASS asteroid classes compared with 3 AhS stones studied here and from [14,15,22]. The 450/550 and 750/550 nm ratios are from [17]. Albedo data for asteroids are at zero phase angle ( $i=0$ ,  $e=0$ ), while AhS samples are at laboratory geometry of  $i=30$ ,  $e=0$ . The meteorites would be slightly brighter at zero phase angle.

**References:** [1] Warren P.H. (2011) *GCA* 75, 6912–6926. [2] Goodrich C.A. et al. (2015) *MAPS* 50, 782–809. [3] Cloutis E. et al. (2010) *MAPS* 45, 10–11. [4] Gillis-Davis J. et al. (2013) *LPS* 44, #2494. [5] Gillis-Davis J. et al. (2015) *LPS* 46, #1607. [6] Gillis-Davis J. et al. (2017) *Icarus*, 10.1016/j.icarus.2016.12.031. [7] Keller L. et al. (2015) *LPI Contrib.* #1878. [8] Hiroi T. and Pieters C.M. (1991) *Proc. LPS* 22, 313–325. [9] Horstmann M. and Bischoff A. (2014) *Chemie der Erde* 74, 149–183. [10] Jenniskens P. et al. (2009) *Nature* 12, 458–488. [11] Kaluna et al. (2016) *Icarus*, 10.1016/j.icarus.2016.12.028. [12] Yamada et al. 1999. *Earth Planet. Space Sci.* 51, 1255–1265. [13] Warren P. and Rubin A. (2010) *GCA* 74, 5109–5133. [14] Hiroi T. et al. (2010) *MAPS* 45, 1836–1845. [15] Goodrich C.A. et al. (2018) *LPS* 49, this meeting. [16] Mittlefehldt D. et al. (1998) *RIM* 36. [17] DeMeo F. et al. (2009) *Icarus* 202, 160–180. [18] Mainzer A. et al. (2011) *Ap. J.* 741(90). [19] Ott U. et al. (2010) *LPS* 41, #1195. [20] Downes H. et al. (2015) *MAPS* 50, 255–272. [22] Goodrich C.A. et al. (2017) *80<sup>th</sup> MSM* #6214.